

Department of Biomechatronics Engineering

College of Bioresources and Agriculture

National Taiwan University

Research Report

Attitude and Angular Velocity Estimation of Surgical Robot Using
Sensor Fusion with Optical Tracker, IMU, and Quaternion-based
Extended Kalman Filter

Wei-Hsuan Cheng

Advisor: Ping-Lang Yen, Ph.D.

October 2023

Abstract

For surgical robots that conduct minimally invasive surgeries, robust and precise perception of the robot end-effector is required for tracking and navigation of the surgical probes or needles. In this scenario, single sensor may not be sufficient due to its natural limitation that reduce the sensing robustness. This leads to the need for sensor fusion, which combines multiple sensory data and generates a better perception of the robot. One of the most common approaches for sensor fusion is the Kalman filter algorithm. In this report, a sensor fusion framework is used for estimating the attitude and angular velocity of robot end-effector in constant angular velocity motion. The multi-sensor system consists of an optical tracker (NDI) and an inertial measurement unit (IMU), and a mathematical model for extended Kalman filter is proposed. Experimental results are shown to verify the proposed model and framework.

Keywords: Surgical Robots, Robot Perception, Attitude and Angular Velocity Estimation, Sensor Fusion, Quaternions, Extended Kalman Filter (EKF), Optical Tracker, Inertial Measurement Unit.

Contents

| | |
|---|-----------|
| 1. Introduction | 4 |
| 1.1 Background and overview..... | 4 |
| 1.2 Objective | 4 |
| 1.3 Literature review | 5 |
| 1.3.1 Sensor fusion and Kalman filter..... | 5 |
| 1.3.2 Quaternions..... | 7 |
| 1.3.3 Quaternion-based extended Kalman filter | 7 |
| 2. Methodology | 9 |
| 2.1 Proposed mathematical model..... | 9 |
| 2.1.1 Notations and symbols..... | 9 |
| 2.1.2 Basic operations of quaternions | 10 |
| 2.1.3 Quaternion kinematics and useful definitions | 11 |
| 2.1.4 Nonlinear state-space model in quaternion-based EKF | 11 |
| 2.1.5 Linearization process..... | 12 |
| 2.1.6 EKF algorithm..... | 12 |
| 3. Experimental results..... | 13 |
| 3.1 Experimental setup and system architecture..... | 13 |
| 3.1.1 Equipment setup..... | 13 |
| 3.1.2 System architecture..... | 13 |
| 3.1.3 Experimental setup | 14 |
| 3.2 Experimental results..... | 15 |
| 4. Conclusion..... | 18 |
| References | 19 |

1. Introduction

1.1 Background and overview

In field of robotic and autonomous systems, there're three typical aspects- perception, planning, and control. Perception- a robot needs to percept the environmental conditions or changes, and extract useful information from them to decide what to do next. Planning, or decision making- a robot needs to be informed of its next step, which can be either a motion predefined by the designer or a decision or path generated by AI. Control- for the plans to be well-executed so that the system behaves exactly like what the designer wants, control strategy should be involved.

Though all of the three above-mentioned aspects are crucial to the system, this text specializes in the perception of a surgical robot, where robust and precise sensing is required in robot-assisted surgeries.

1.2 Objective

For surgical robots (figure 1) [13: P.-L. Yen, et al. 2021], robust and precise sensing/estimation of attitude and angular velocity of the end-effector is required for conducting robot-assisted minimally invasive surgeries. To increase the robustness of sensor system, sensor fusion technique can be used accompanied by estimation algorithms, such as Kalman filtering. These builds up a more robust and precise perception of the robot, which is essential for further stages such as motion planning, navigation, or control, etc.

In this report, a sensor fusion framework is proposed for the estimation of attitude and angular velocity of the robot end-effector which is in the motion of constant angular velocity. The multi-sensor system consists of an optical tracker system (NDI) and an inertial measurement unit (IMU); a quaternion-based extended Kalman filter algorithm is proposed for estimation. The NDI has a strength of high accuracy, yet has low measurement frequency, limited measuring volume and is vulnerable to marker occlusions. IMU, on the other hand, has high measurement frequency, unlimited measuring volume, while suffers from low accuracy, high noise, and DC bias problems [2: Oh, H., et al. 2015]. The two sensors are complementary to each other and the fusion of two sensory data combined with an estimation algorithm can generate a robust and optimal estimation of the robot state.

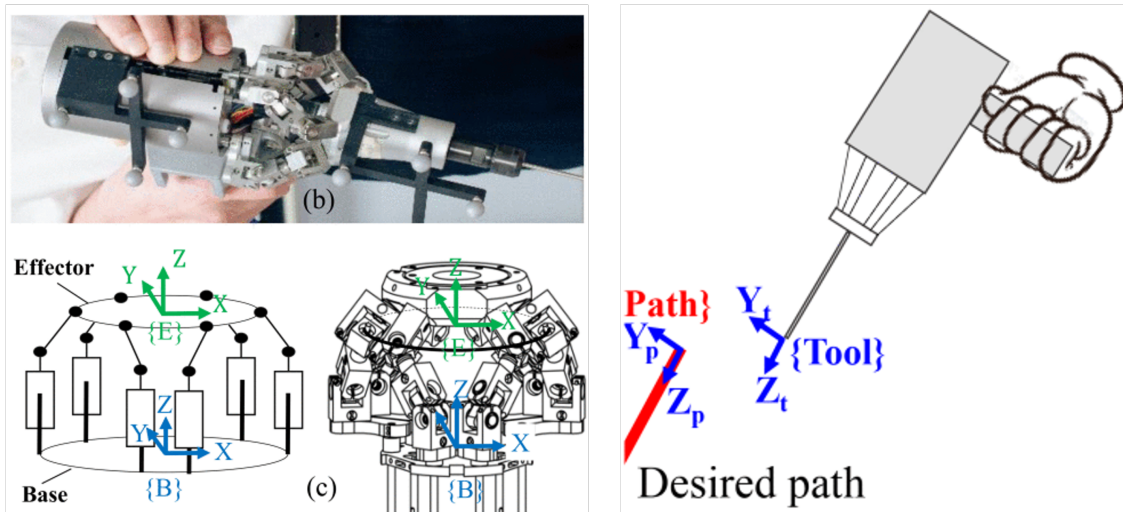


Figure 1 Surgical robot and its end-effector [13: P.-L. Yen, et al. 2021]

1.3 Literature review

1.3.1 Sensor fusion and Kalman filter

Sensor fusion is a well-known method that “fuses” multiple sensory signals (often provided by multiple sensors together) to generate a more consistent, accurate, dependable, and robust sensing information. Sensor fusion brings various advantage to the perception of the system such as higher robustness and reliability, extended spatial and temporal coverage, higher resolution, less ambiguity and uncertainty, etc. [1: W. Elmenreich, 2002].

One of the most common approaches for sensor fusion in existing literature is the Kalman filter, which is an algorithm that combines mathematical model and (multi-)sensor measurements, and then optimally estimate the system’s state. [2: Oh, H., et al. 2015] proposed a sensor fusion framework with NDI and IMU based on Kalman filter to estimation the attitude of surgical instruments (figure 2). While it is specific for attitude estimation, not including angular velocity. [3: L. Armesto, et al. 2004] proposed a mathematical model for multi-rate sensor fusion based on extended and unscented Kalman filter; vision sensor and inertia sensor are utilized. The state equation in the proposed model is a 6D tracking system, which, instead of rotation matrices, uses quaternions to describe attitude.

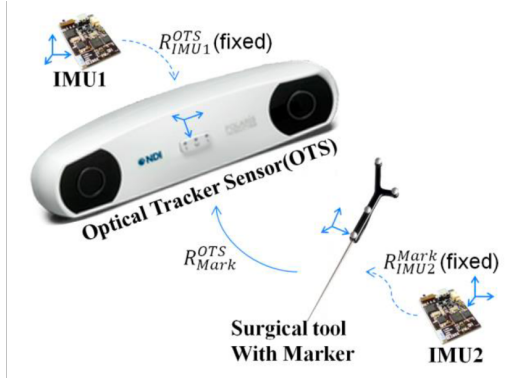


Figure 2 Sensor fusion with NDI and IMU [2: Oh, H., et al. 2015]

1.3.2 Quaternions

Quaternions can be used to describe rigid body attitude and rotation in 3D space. There're numerous advantages of using quaternions instead of rotation matrices to describe rotations. For example, as describing 3D rotations, rotation matrices have 9 parameters due to their nature of matrix algebra; while, quaternions only have 4 parameters and thus are minimally parameterized, and thus having higher computational efficiency, as compared to rotation matrices [4: J. Sola, 2017]. Literature also shows that for the feedback for spacecraft attitude stabilization, quaternions perform better than rotation matrices both in terms of speed of convergence and of energy consumption [5: Celani F., 2022]. There're plenty of advantage of using quaternions rather than rotation matrices, a more detailed comparison of these two is given in [6: Hans-Peter Schröcker, 2022].

1.3.3 Quaternion-based extended Kalman filter

To describe the attitude of a rigid body, rotational motion should be involved; while, rotations are nonlinear in general, which exceed the scope of

what a Kalman filter is able to describe. Therefore, an extended Kalman filter (EKF) is an extension of Kalman filter that is valid for describing nonlinear system through linearization process at each time sample.

According to existing literature, there're many proposed models for quaternion-based extended Kalman filter, each with slight differences, depending on the application scenarios. [3: L. Armesto, et al. 2004] proposed a 6D tracking model for EKF, where three of the six dimensions are to describe rotational motion and is parameterized by quaternions. Though that the discrete-time propagation of quaternions is given, the whole model for EKF is not shown explicitly. [4: J. Sola, 2017] proposed a model for extended Kalman filter that involves both quaternions and rotation matrices in the states. The state vector is defined using the error states of the system. [7: H. Himberg, et al. 2009] proposed a simple model for EKF that can estimate head orientation and head angular velocity using the approximated solution of quaternion discrete-time propagation.

In this report, a model for quaternion-based EKF using an analytical solution of quaternion propagation equation is proposed. The model is similar to the rotation part in [3: L. Armesto, et al. 2004], but with slight differences in the quaternion propagation equation. Detailed math equations of the model are also provided in this text. The proposed model is verified through physical experiment.

2. Methodology

2.1 Proposed mathematical model

2.1.1 Notations and symbols

1. (\cdot) (No special symbols): Scalar.
2. $\vec{(\cdot)}$ (Vector symbol): Vector.
3. \mathbf{q} (Boldface): Quaternion (4-vector).
4. \mathbf{q}^* (Asterisk): Quaternion conjugation.
5. q_0 : Scalar part of the quaternion.
6. \vec{q} : Vector part of the quaternion.
7. $(\cdot)_n$: The n th entry of the quaternion or vector.
8. $\cdot \cdot$: Dot product.
9. \times : Cross product.
10. \otimes : Quaternion product.
11. $[(\cdot)]_\times$: Skew- (cross-product-) operator.
12. $[(\cdot)\otimes]$: Left-quaternion-product matrix.
13. $[(\cdot)\odot]$: Right-quaternion-product matrix.
14. T_s, f_s : Discrete-time sampling period and sampling rate.
15. $\hat{(\cdot)}$ (Hat): State estimate.

2.1.2 Basic operations of quaternions

1. Quaternion definition

$$\begin{aligned} \mathbf{q} &= q_0 + q_1 i + q_2 j + q_3 k \in \mathbb{H}, q_n \in \mathbb{R}, \forall n \\ &:= \underbrace{q_0}_{\in \mathbb{R} \subset \mathbb{H} \text{ (scalar part)}} + \underbrace{\vec{q}}_{\in \mathbb{H}_p \subset \mathbb{H} \text{ (vector part)}} \equiv \begin{bmatrix} q_0 \\ \vec{q} \end{bmatrix} \text{ (represented in 4-vector)}, \\ i^2 &= j^2 = k^2 = ijk = -1. \end{aligned} \quad (1)$$

2. Quaternion product (non-commutative in general)

$$\mathbf{q} \otimes \mathbf{p} = (q_0 p_0 - \vec{q} \cdot \vec{p}) + (q_0 \vec{p} + p_0 \vec{q} + \vec{q} \times \vec{p}) \equiv \begin{bmatrix} q_0 p_0 - \vec{q} \cdot \vec{p} \\ q_0 \vec{p} + p_0 \vec{q} + \vec{q} \times \vec{p} \end{bmatrix} \quad (2)$$

3. Unit quaternion

$$\|\mathbf{q}\| := \sqrt{\mathbf{q} \otimes \mathbf{q}^*} = \sqrt{\sum_n q_n^2} = 1. \quad (3)$$

4. Unit quaternion as a rotator (rotate around the unit vector \vec{u} by an angle θ), as shown in figure 3,

$$\mathbf{q} := e^{\frac{\theta}{2} \mathbf{u}} = \cos \frac{\theta}{2} + \vec{u} \sin \frac{\theta}{2} \equiv \begin{bmatrix} \cos \frac{\theta}{2} \\ \vec{u} \sin \frac{\theta}{2} \end{bmatrix}, \mathbf{u} := \begin{bmatrix} 0 \\ \vec{u} \end{bmatrix}, \quad (4)$$

where $e^{(\cdot)}$ is defined using the *Euler's formula*, viz, $e^{(\cdot)} = 1 + (\cdot) + \frac{1}{2!}(\cdot) \otimes (\cdot) + \frac{1}{3!}(\cdot) \otimes (\cdot) \otimes (\cdot) + \dots$.

5. The rotation action (rotate a vector \vec{p} using the *sandwich product*)

$$\mathbf{p}' = \mathbf{q} \otimes \mathbf{p} \otimes \mathbf{q}^*, \mathbf{p} =: \begin{bmatrix} 0 \\ \vec{p} \end{bmatrix}. \quad (5)$$

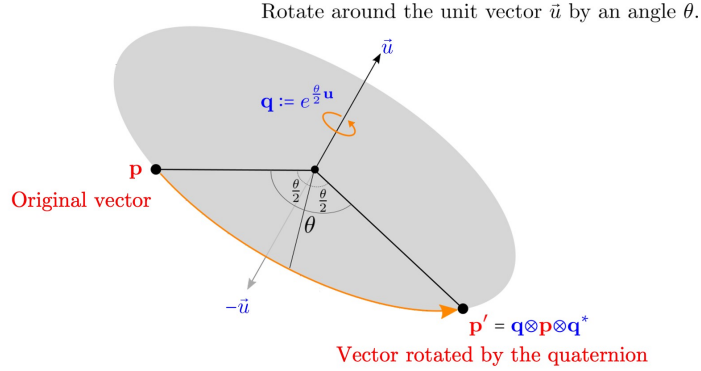


Figure 3 Quaternion as a rotator [8: Song Ho Ahn]

2.1.3 Quaternion Kinematics and useful definitions

Considering the angular velocity and quaternion $\vec{\omega} = [\omega_x \ \omega_y \ \omega_z]^T$, $\boldsymbol{\omega} := \begin{bmatrix} 0 \\ \vec{\omega} \end{bmatrix}$, $\mathbf{q} \equiv \begin{bmatrix} q_0 \\ \vec{q} \end{bmatrix}$, the following definitions are given [4: J. Sola, 2019] [9: F. L. Markley, et al. 2014].

1. Skew-Operator $[(\cdot)]_\times$

$$[\vec{\omega}]_\times := \begin{bmatrix} 0 & -\omega_z & \omega_y \\ \omega_z & 0 & -\omega_x \\ -\omega_y & \omega_x & 0 \end{bmatrix} \in \mathbb{R}^{3 \times 3}, \text{ s.t. } \vec{\omega} \times (\cdot) = [\vec{\omega}]_\times(\cdot) \quad (6)$$

2. Left- and Right- Quaternion-Product Matrices, $[(\cdot)\otimes]$, $[(\cdot)\odot]$

$$[\mathbf{q}\otimes] := q_0 I + \begin{bmatrix} 0 & -\vec{q}^T \\ \vec{q} & [\vec{q}]_\times \end{bmatrix} \in \mathbb{R}^{4 \times 4}, \text{ s.t. } \mathbf{q} \otimes (\cdot) \equiv [\mathbf{q}\otimes](\cdot), \quad (7)$$

$$[\mathbf{q}\odot] := q_0 I + \begin{bmatrix} 0 & -\vec{q}^T \\ \vec{q} & -[\vec{q}]_\times \end{bmatrix} \in \mathbb{R}^{4 \times 4}, \text{ s.t. } (\cdot) \otimes \mathbf{q} \equiv [\mathbf{q}\odot](\cdot) \quad (8)$$

3. Left-Quaternion-Product Matrix of $\vec{\omega}$

$$\Omega(\vec{\omega}) := [\boldsymbol{\omega}\otimes]. \quad (9)$$

Followed by (6)-(9), the quaternion can be derived,

1. Quaternion ODE (Quaternion Kinematics) (Derived using (7)-(9), and [10: Y.-B. Jia, 2015])

$$\dot{\mathbf{q}}(t) = \frac{1}{2} \boldsymbol{\omega}(t) \otimes \mathbf{q}(t) \equiv \frac{1}{2} \Omega(\vec{\omega}(t)) \mathbf{q}(t). \quad (10)$$

2. Quaternion Propagation in Discrete-Time (Derived using (10), [9: F. L. Markley, et al. 2014], and [11: D. Simon, 2006])

$$\mathbf{q}(k+1) = e^{\frac{T_s}{2} \boldsymbol{\omega}(k)} \otimes \mathbf{q}(k) \equiv \underbrace{\left[\cos\left(\frac{T_s}{2} \|\vec{\omega}(k)\| \right) I + \frac{1}{\|\vec{\omega}(k)\|} \sin\left(\frac{T_s}{2} \|\vec{\omega}(k)\| \right) \Omega(\vec{\omega}(k)) \right]}_{:=g(k, \vec{\omega}(k)): \mathbb{R} \times \mathbb{R}^3 \rightarrow \mathbb{R}^{4 \times 4}} \mathbf{q}(k), \quad (11)$$

which is a closed-form solution if $\vec{\omega}$ is const. or holds const. over each sampling period.

2.1.4 Nonlinear state-space model in quaternion-based EKF

Define the system state x , process noise w , output measurement z , and measurement noise v ,

$$x(k) := \begin{bmatrix} \mathbf{q}(k) \\ \vec{\omega}(k) \\ \vec{\omega}_b(k) \end{bmatrix}, x : \mathbb{R} \rightarrow \mathbb{R}^{10}; w(k) := \begin{bmatrix} w_{\mathbf{q}}(k) \\ \vec{\alpha}(k) \\ \vec{\alpha}_b(k) \end{bmatrix}, w : \mathbb{R} \rightarrow \mathbb{R}^{10}, w(k) \sim \mathcal{N}(0, \Sigma_w(k)); \quad (12)$$

$$z(k) := \begin{bmatrix} \mathbf{q}_m(k) \\ \vec{\omega}_m(k) \end{bmatrix}, z : \mathbb{R} \rightarrow \mathbb{R}^7; v(k) := \begin{bmatrix} v_{\mathbf{q}_m}(k) \\ v_{\vec{\omega}_m}(k) \end{bmatrix}, v : \mathbb{R} \rightarrow \mathbb{R}^7, v(k) \sim \mathcal{N}(0, \Sigma_v(k)), \quad (13)$$

where the system state consists of the quaternion \mathbf{q} , angular velocity $\vec{\omega}$, and its bias $\vec{\omega}_b$. \mathbf{q}_m and $\vec{\omega}_m$ are quaternion measurement and angular velocity measurements, obtained from optical tracker (NDI) and IMU, respectively; $\vec{\omega}_b$ is the angular velocity bias of IMU; $w(k)$ and $v(k)$ are process and measurement noises, both are white, zero-mean, Gaussian stochastic processes.

Combining (11)-(13) and assuming constant angular velocity and bias yields,

$$\begin{bmatrix} \mathbf{q}(k+1) \\ \vec{\omega}(k+1) \\ \vec{\omega}_b(k+1) \end{bmatrix} = \begin{bmatrix} g(k, \vec{\omega}(k))\mathbf{q}(k+1) \\ \vec{\omega}(k) \\ \vec{\omega}_b(k) \end{bmatrix} + T_s \cdot \begin{bmatrix} w_{\mathbf{q}}(k) \\ \vec{\alpha}(k) \\ \vec{\alpha}_b(k) \end{bmatrix}, \text{ or } x(k+1) = f(k, x(k)) + \Gamma w(k), \quad (14)$$

$$\begin{bmatrix} \mathbf{q}_m(k) \\ \vec{\omega}_m(k) \end{bmatrix} = \begin{bmatrix} I_{4 \times 3} & 0_{4 \times 3} & 0_{4 \times 3} \\ 0_{3 \times 4} & I_{3 \times 3} & I_{3 \times 3} \end{bmatrix} \begin{bmatrix} \mathbf{q}(k) \\ \vec{\omega}(k) \\ \vec{\omega}_b(k) \end{bmatrix} + \begin{bmatrix} v_{\mathbf{q}_m}(k) \\ v_{\vec{\omega}_m}(k) \end{bmatrix}, \text{ or } z(k) = Hx(k) + v(k) \quad (15)$$

2.1.5 Linearization process

The linearization process in EKF [12: T. Kailath, et al. 2000] requires the computation of Jacobian matrix of the nonlinear function f in (14), which is given by,

$$F_k = \left[\frac{\partial f_i}{\partial x_j} \right]_{x=x(k)} = \begin{bmatrix} g_{4 \times 4} & \left[\frac{\partial(g\mathbf{q})}{\partial \vec{\omega}} \right]_{4 \times 3} & 0_{4 \times 3} \\ 0_{3 \times 4} & I_{3 \times 3} & 0_{3 \times 3} \\ 0_{3 \times 4} & 0_{3 \times 3} & I_{3 \times 3} \end{bmatrix}_{x=x(k)} \in \mathbb{R}^{10 \times 10}, \quad (16)$$

where

$$\left[\frac{\partial(g\mathbf{q})}{\partial \vec{\omega}} \right] = -\frac{T_s}{2\|\vec{\omega}\|} \sin\left(\frac{T_s}{2}\|\vec{\omega}\|\right) \mathbf{q} \vec{\omega}^T + \begin{bmatrix} -\vec{q}^T \\ q_0 I - [\vec{q}]_\times \end{bmatrix} \left\{ \left[\frac{T_s \cos\left(\frac{T_s}{2}\|\vec{\omega}\|\right)}{2\|\vec{\omega}\|} - \frac{\sin\left(\frac{T_s}{2}\|\vec{\omega}\|\right)}{\|\vec{\omega}\|^3} \right] \vec{\omega} \vec{\omega}^T + \frac{\sin\left(\frac{T_s}{2}\|\vec{\omega}\|\right)}{\|\vec{\omega}\|} I \right\}. \quad (17)$$

2.1.6 EKF algorithm

Since all the functions and matrices of the model are already given, the EKF algorithm can be implemented, which is divided into 3 steps [12: T. Kailath, et al. 2000],

- Step 1: Initialization**

Given $\hat{x}(0)$, $P(0)$, $Q(k)$, $R(k)$, where $Q(k) = \Gamma \Sigma_w(k) \Gamma^T$, $R(k) = \Sigma_v(k)$.

- Step 2: Prediction**

A priori estimation: state \hat{x}^- and error covariance P^-

$$\begin{cases} \hat{x}^-(k+1) = f(k, \hat{x}(k)) \\ P^-(k+1) = F_k P(k) F_k^T + Q(k) \end{cases} \begin{array}{l} \text{-State estimate extrapolation (nonlinear)} \\ \text{-Error covariance extrapolation (linear)} \end{array}$$

- Step 3: Update**

A posteriori estimation: state \hat{x} and error covariance P

$$K(k+1) = P^-(k) H^T (H P^-(k) H^T + R(k))^{-1} \text{ - Kalman gain matrix,}$$

$$\begin{cases} \hat{x}(k+1) = \hat{x}^-(k+1) + K(k+1)[z(k+1) - H \hat{x}^-(k+1)] \\ P(k+1) = (I - K(k+1) H) P^-(k+1) \end{cases} \begin{array}{l} \text{-State estimate observational update} \\ \text{-Error covariance update.} \end{array}$$

- Return the state estimate \hat{x} .

3. Experimental results

3.1 Experimental setup and system architecture

3.1.1 Equipment setup

The multi-sensor system consists of an optical tracker (NDI) and an IMU.

The equipment setup is shown in figure 4. The NDI provides quaternion attitude measurement of the marker frames, where each frame is formed by four passive marker spheres. The IMU provides angular velocity measurement.

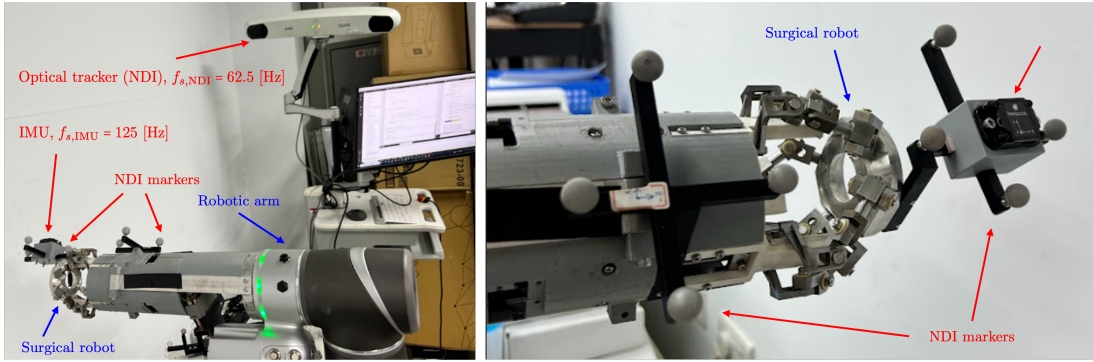


Figure 4 Equipment setup

3.1.2 System architecture

The EKF algorithm is offline-implemented in MATLAB after collecting experimental data. Frame transformation process is done before the algorithm. For the rate of sensors and algorithm, the NDI and IMU has sampling period of 16 ms and 8 ms, respectively; thus, zero-order hold method is chosen and the sampling period of the EKF algorithm is set as 16 ms (, or 62.5 Hz). The system architecture and the block diagram for EKF algorithm are shown in figure 5 and 6.

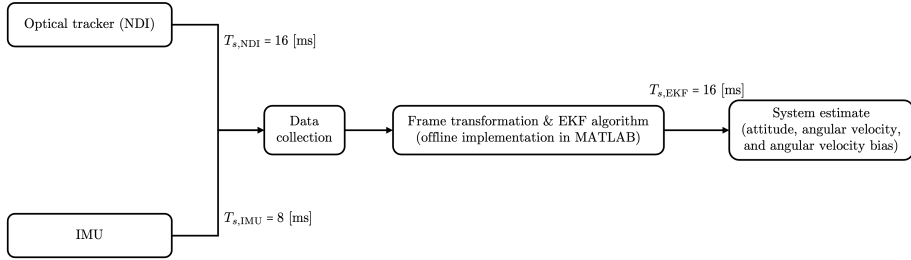


Figure 5 System architecture

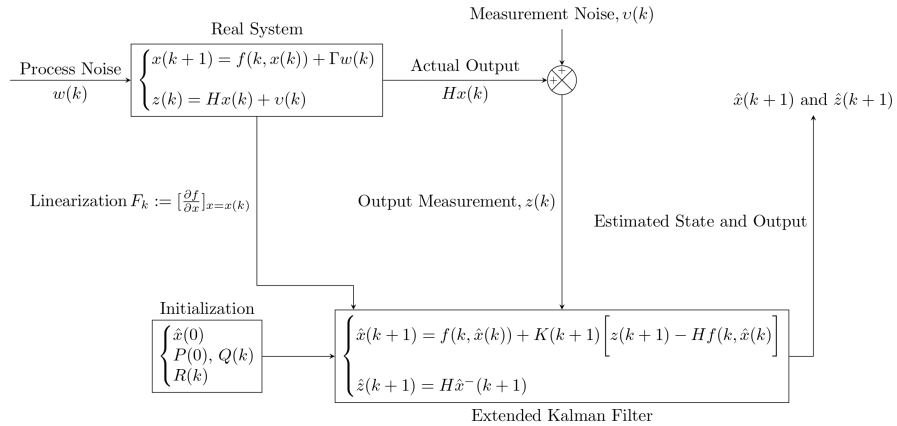


Figure 6 Block diagram for EKF algorithm

3.1.3 Experimental setup

The experiment is conducted in the working volume of NDI, where the angular velocity is set as a constant of **-9 deg/s** with respect to the x-axis of the marker mounted on the surgical robot's end-effector. The marker has no relative motion with respect to the end-effector. Then, the frame transformation process is done by transforming all the frames as with respect to the initial pose of that marker, as shown in figure 7. Throughout this, the attitude and angular velocity of the robot's end-effector can be estimated and treated the same as those of the marker frame. Apart from NDI and IMU that are involved in the algorithm, the encoder of the robot

joint is set as the ground-truth of the experiment. Results of the experiment are shown in next subsection.

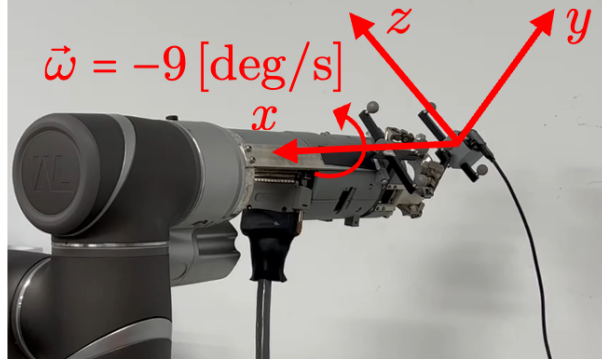


Figure 7 Experimental setup

3.2 Experimental results

The experimental results of the attitude and angular velocity estimation using quaternion-based extended Kalman filter are shown in the below figures. Figure 8 and 9 show the estimate of quaternion attitude and angular velocity of the robot end-effector; the measurement and ground-truth value are also shown. Figure 10 shows the estimate of the angular velocity bias of the robot end-effector as compared to its measurement value when the robot is at rest initially.

The algorithm also increases the robustness of the estimates against occlusions. Figure 11 shows the results as a 0.5 [s] sudden occlusion occurs. The measurements of attitude and angular velocity are being zero-order held, while the estimate remains. Figure 12 is a 3D plot that demonstrate the rotational motion of the marker frame (as well as the end-effector). It can be seen in these figures that the proposed sensor fusion framework better estimate the system state, which is comprised of the attitude and the

angular velocity of the robot end-effector. The EKF provides estimates that are either smoother, or closer to ground-truth, or both, and thus, leads to a more robust (against occlusions) and precise perception of the surgical robot system.

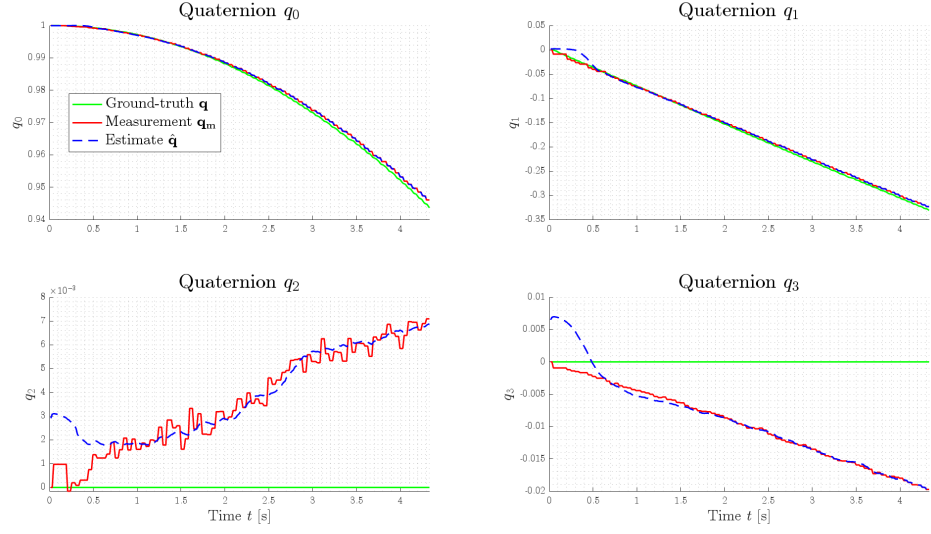


Figure 8 Quaternion attitude estimate, measurement, and ground truth

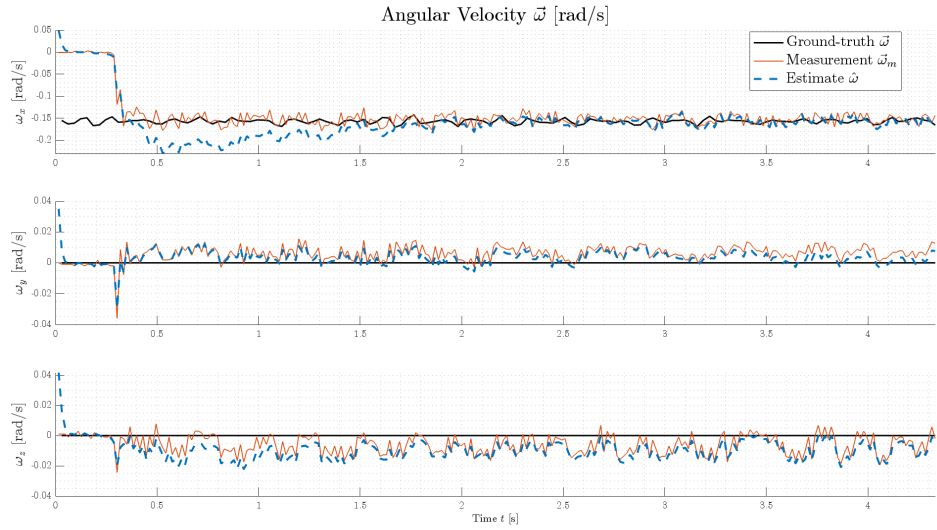


Figure 9 Angular velocity estimate, measurement, and ground truth

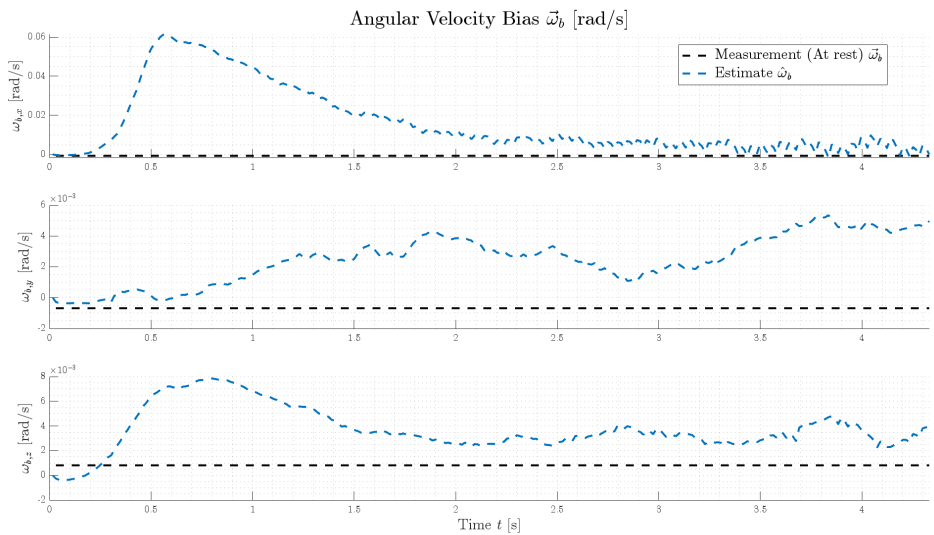
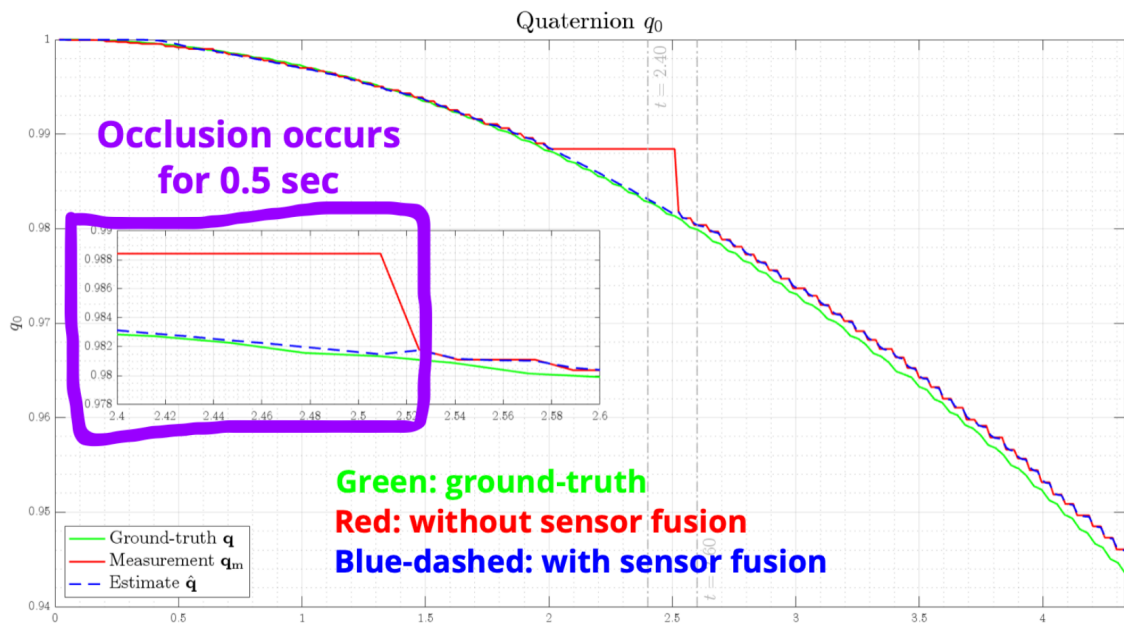


Figure 10 Angular velocity bias estimate, and measurement at rest



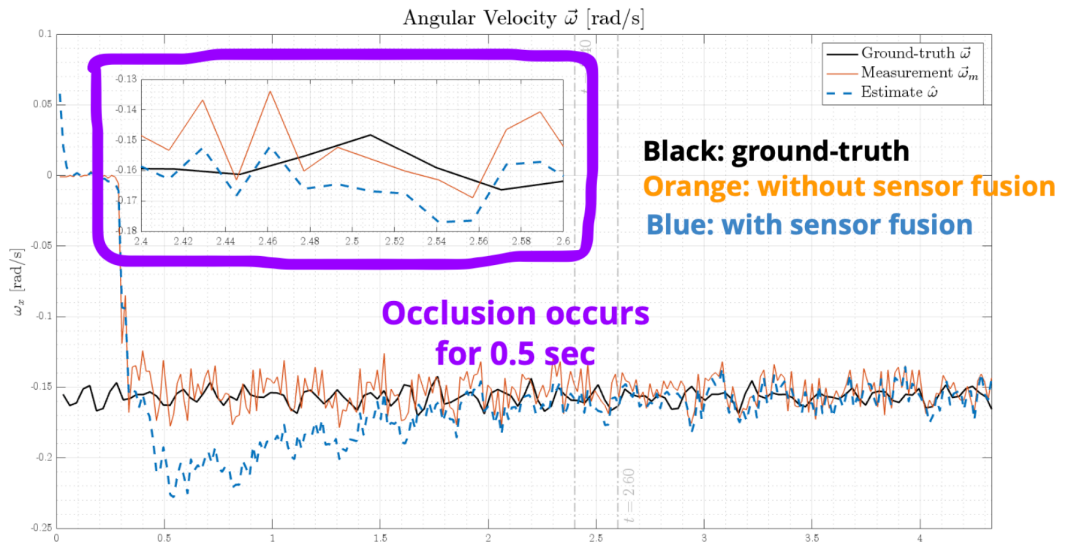


Figure 11 Robustness evaluation against sudden occlusions. Zero-order hold for measurements during the 0.5 [s] occlusions. Attitude estimate (left) and angular velocity estimate (right).

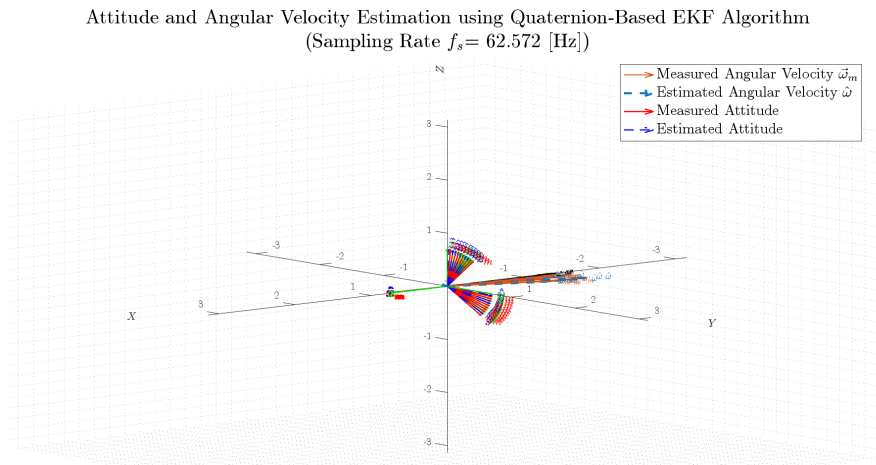


Figure 12 3D demonstration of rotational motion of the marker frame

4. Conclusion

In this work, a sensor fusion framework using quaternion-based extended Kalman filter is proposed for increasing the robustness and precision of the surgical robot's perception. A mathematic model involving quaternion attitude and angular velocity is proposed and implemented in the EKF algorithm, with the sensor system constructed by an optical tracker (NDI) and an inertial measurement unit (IMU). Experimental results show that the EKF algorithm fusing the 2 sensory information with the knowledge of system model, acts as an optimal estimator as well as a filter, which gives a more smooth and accurate estimate value for the system state. The experiment is conducted offline and implemented in MATLAB, and it can be further implemented in C++ or Python for real-time estimation in the future.

References

- [1] W. Elmenreich, "Sensor fusion in time-triggered systems", 2002.
- [2] Oh, H.; Chae, Y.; An, J.; Kim, M. Pose estimation of surgical instrument using sensor data fusion with optical tracker and IMU based on Kalman filter. MATEC Web Conf. 2015, 32, 04008.
- [3] L. Armesto, S. Chroust, M. Vincze and J. Tornero, "Multi-rate fusion with vision and inertial sensors", *Proc. IEEE Int. Conf. Robot. Autom.*, pp. 193-199, 2004.
- [4] J. Sola, "Quaternion kinematics for the error-state kalman filter", 2017.
- [5] Celani F., "Quaternion versus rotation matrix feedback for spacecraft attitude stabilization using magnetorquers". Aerospace, 9 (1) (2022), p. 24.
- [6] Hans-Peter Schröcker, "Quaternions as a Riemannian Manifold." IROS'22 Tutorial "Riemann and Gauss meet Asimov: A tutorial on geometric methods in robot learning, optimization, and control.
- [7] H. Himberg and Y. Motai, "Head orientation prediction: Delta quaternions versus quaternions", IEEE Trans. Syst. Man Cybern. B Cybern., vol. 39, no. 6, pp. 1382-1392, Dec. 2009.
- [8] Song Ho Ahn, http://www.songho.ca/opengl/gl_quaternion.html.
- [9] F. L. Markley and J. L. Crassidis, Fundamentals of Spacecraft Attitude Determination and Control, New York, NY, USA:Springer, vol. 33, 2014.
- [10] Y.-B. Jia, "Quaternions", Course Com S, vol. 477, pp. 577, 2019.
- [11] D. Simon, Optimal State Estimation: Kalman H Infinity and Nonlinear Approaches, NJ, Hoboken:Wiley, 2006.
- [12] T. Kailath, A. H. Sayed and B. Hassibi, Linear Estimation, Upper Saddle

River, NJ, USA:Prentice-Hall, 2000.

- [13] P.-L. Yen and T.-H. Ho, "Shared control for a handheld orthopedic surgical robot", *IEEE Robot. Automat. Lett.*, vol. 6, no. 4, pp. 8394-8400, Oct. 2021.